

# Volumetric assessment of recurrent or progressive gliomas: comparison between F-DOPA PET and perfusion-weighted MRI

Francesco Cicone · Christian P. Filss · Giuseppe Minniti · Camilla Rossi-Espagnet · Annalisa Papa · Claudia Scaringi · Norbert Galldiks · Alessandro Bozzao · N. Jon Shah · Francesco Scopinaro · Karl-Josef Langen

Received: 11 December 2014 / Accepted: 5 February 2015 / Published online: 7 March 2015  
© Springer-Verlag Berlin Heidelberg 2015

## Abstract

**Purpose** To compare the diagnostic information obtained with 6- $^{18}\text{F}$ -fluoro-L-3,4-dihydroxyphenylalanine (F-DOPA) PET and relative cerebral blood volume (rCBV) maps in recurrent or progressive glioma.

**Methods** All patients with recurrent or progressive glioma referred for F-DOPA imaging at our institution between May 2010 and May 2014 were retrospectively included, provided

that macroscopic disease was visible on conventional MRI images and that rCBV maps were available for comparison. The final analysis included 50 paired studies (44 patients). After image registration, automatic tumour segmentation of both sets of images was performed using the average signal in a large reference VOI including grey and white matter multiplied by 1.6. Tumour volumes identified by both modalities were compared and their spatial congruence calculated. The distances between F-DOPA uptake and rCBV hot spots, tumour-to-brain ratios (TBRs) and normalized histograms were also computed.

**Results** On visual inspection, 49 of the 50 F-DOPA and 45 of the 50 rCBV studies were classified as positive. The tumour volume delineated using F-DOPA ( $\text{F-DOPA}_{\text{vol } 1.6}$ ) greatly exceeded that of rCBV maps ( $\text{rCBV}_{\text{vol } 1.6}$ ). The median  $\text{F-DOPA}_{\text{vol } 1.6}$  and  $\text{rCBV}_{\text{vol } 1.6}$  were 11.44 ml (range 0–220.95 ml) and 1.04 ml (range 0–26.30 ml), respectively ( $p < 0.00001$ ). Overall, the median overlapping volume was 0.27 ml, resulting in a spatial congruence of 1.38 % (range 0–39.22 %). The mean hot spot distance was 27.17 mm ( $\pm 16.92$  mm). F-DOPA uptake TBR was significantly higher than rCBV TBR ( $1.76 \pm 0.60$  vs.  $1.15 \pm 0.52$ , respectively;  $p < 0.0001$ ). The histogram analysis showed that F-DOPA provided better separation of tumour from background. In 6 of the 50 studies (12 %), however, physiological uptake in the striatum interfered with tumour delineation.

**Conclusion** The information provided by F-DOPA PET and rCBV maps are substantially different. Image interpretation is easier and a larger tumour extent is identified on F-DOPA PET images than on rCBV maps. The clinical impact of such differences needs to be explored in future studies.

**Keywords** Glioma · Amino acid brain PET · DOPA · Tumour volume · rCBV maps · Perfusion-weighted magnetic resonance

Francesco Cicone and Christian P. Filss contributed equally to this work.

F. Cicone (✉) · A. Papa · F. Scopinaro  
Unit of Nuclear Medicine, Sant'Andrea Hospital, Rome, Italy  
e-mail: f.cicone@ioli.it

F. Cicone · G. Minniti · A. Papa · C. Scaringi · F. Scopinaro  
Department of Surgical and Medical Sciences and translational Medicine, Faculty of Medicine and Psychology, "Sapienza" University of Rome, Rome, Italy

F. Cicone · C. P. Filss · N. Galldiks · N. J. Shah · K.-J. Langen  
Institute of Neuroscience and Medicine, Research Centre Juelich, Juelich, Germany

C. P. Filss · K.-J. Langen  
Department of Nuclear Medicine, RWTH Aachen University Hospital, Aachen, Germany

G. Minniti · C. Scaringi  
Unit of Radiotherapy, Sant'Andrea Hospital, Rome, Italy

C. Rossi-Espagnet · A. Bozzao  
Unit of Neuroradiology, Sant'Andrea Hospital, Rome, Italy

C. Rossi-Espagnet · A. Bozzao  
Department of Neurosciences, Mental Health and Sensory Organs (Ne.S.M.O.S.), Faculty of Medicine and Psychology, "Sapienza" University of Rome, Rome, Italy

N. Galldiks  
Department of Neurology, University of Cologne, Cologne, Germany

## Introduction

Structural magnetic resonance imaging (MRI) is the current standard for detection and follow-up of brain tumours of any grade and histology. However, conventional contrast-enhanced T1-weighted (ce-T1-W) and fluid-attenuated inversion recovery (FLAIR) sequences have well known limitations especially in the evaluation of posttreatment changes. Response assessment criteria are therefore evolving over time in consideration of the issues raised by new optimized radiotherapy and chemotherapy protocols [1]. The need for additional insights into tumour biology and infiltration has prompted the increasing use of radionuclide PET imaging and advanced MRI techniques, such as perfusion-weighted and diffusion-weighted MRI (PWI, DWI) and proton spectroscopy [2, 3].

Among the positron-emitting radiotracers, amino acid probes including L-[methyl- $^{11}\text{C}$ ]methionine (MET), O-(2- $^{18}\text{F}$ -fluoroethyl)-L-tyrosine (FET) and 6-[ $^{18}\text{F}$ ]-fluoro-L-3,4-dihydroxyphenylalanine (F-DOPA) have been most successful in the field of brain tumour imaging due to their favourable mechanism of uptake, that depends on the increased expression of the L-type amino acid transport system on tumour cells [4]. This metabolic pathway is highly specific for cancer cells and largely independent of blood–brain barrier breakdown, resulting in excellent tumour-to-background contrast. Pathological amino acid uptake usually extends beyond ce-T1-W abnormalities and is more specific than T2-weighted (or FLAIR) hyperintensities [5]. The inclusion of amino acid PET tracers in the work-up of brain tumours complements and improves the diagnostic performances of conventional MRI in several settings, including biopsy targeting [6–8], prediction of anaplastic transformation [9, 10], response assessment [11–13] and treatment planning [14–16] for both high-grade and low-grade gliomas.

In addition, advanced MRI sequences such as dynamic susceptibility-weighted contrast-enhanced perfusion (DSC-PWI) have been proposed as a useful complement to conventional MRI, both in the preoperative setting [17] and in response evaluation [18, 19]. Relative cerebral blood volume (rCBV), the most informative parameter derived from PWI images, increases with microvessel density and angiogenesis, and correlates with tumour grade and proliferation [20, 21]. Despite inherent technical and biological differences between the two imaging modalities, several authors have claimed that the diagnostic information provided by PWI is comparable, or even superior, to that obtained by amino acid PET [22–25]. A recent study in patients with brain tumours showed considerably higher tumour-to-brain ratios (TBR) and larger tumour volumes on FET PET as well as a poor spatial overlap compared with PWI [26]. So far, no previous studies have evaluated differences between F-DOPA uptake and rCBV maps in patients with gliomas. Therefore the present study was

designed to compare the diagnostic information obtained with F-DOPA PET and rCBV maps in a large unselected population of patients with recurrent or progressive gliomas, with particular focus on volumetric comparison and spatial congruence analysis. In order to ensure comparability, the same methodology of the previous study comparing FET PET and PWI was used [26].

## Materials and methods

### Patients

A total of 62 F-DOPA PET studies from 55 patients (19 women and 36 men; median age 50 years, range 19 – 79 years) acquired between May 2010 and May 2014 at Sant'Andrea University Hospital of Rome were selected from a prospectively maintained database of patients with brain tumours treated at the same institution. Patients were included in this retrospective analysis if they presented with recurrent or progressive disease at the time of PET scan visible on standard T1-weighted and/or FLAIR MRI sequences, according to the RANO criteria [1]. Twelve studies were excluded because PWI MRI was not available for review and/or MRI and F-DOPA PET were not acquired within a short time of each other, i.e. no longer than 3 and 6 weeks apart for high-grade and low-grade gliomas, respectively. Therefore, a dataset of 50 F-DOPA PET scans from 44 patients (16 women, 28 men) were entered into the final analysis.

At the time of PET imaging, diagnoses were defined according to the World Health Organization (WHO) classification [27]. High-grade gliomas (36 studies) included grade IV glioblastomas (19 studies, 15 de novo and 4 secondary), grade III anaplastic astrocytomas (10 studies), grade III anaplastic oligoastrocytomas (2 studies), a grade III anaplastic oligodendroglioma (1 study), a grade III ganglioglioma (1 study), and grade III gliomatosis cerebri (3 studies; defined by the presence of tumour tissue in at least three cerebral lobes). There were 14 low-grade gliomas, including grade II diffuse astrocytomas (5 studies), grade II oligodendrogliomas (5 studies), and a WHO grade II oligoastrocytoma (1 study). There were three histologically unverified noncontrast-enhancing diffuse pontine gliomas.

All patients had received previous treatment, including surgical resection, radiotherapy, chemotherapy or a combination thereof. Total, subtotal and partial resection were defined as complete removal, removal of >90 % and removal of <90 % of the tumour, respectively, evaluated on postoperative MRI performed within the first 24 h. Radiotherapy was delivered at a total dose of 59.4 – 60 Gy in 30 – 33 fractions of 1.8 – 2.0 Gy each. Chemotherapy consisted of concomitant (75 mg/m<sup>2</sup> daily) and/or adjuvant (150 – 200 mg/m<sup>2</sup> for 5 days every

28 days) temozolomide [28]. Of the 44 patients, 25 (a total of 28 paired imaging studies) were on temozolomide chemotherapy as part of their primary treatment or for progressive disease. None of the patients had previously received antiangiogenic treatment.

#### F-DOPA PET and MRI imaging protocols

One 20-min static image of the brain was acquired on a Philips Gemini PET/CT camera starting  $15 \pm 5$  min after intravenous injection of 185 MBq (range 148 – 196 MBq)  $^{18}\text{F}$ -DOPA. Patients were required to fast for at least 6 h before the scan and no carbidopa premedication was given. A low-dose, noncontrast-enhanced CT scan (120 kV, 60 mA) was acquired for attenuation correction. Images were reconstructed using a 3D RAMLA algorithm on a  $128 \times 128$  matrix and a square field of view (FOV) of 256 mm side, yielding a final voxel of  $8 \text{ mm}^3$ .

All MRI scans were performed on a 1.5-T unit (Sonata, Siemens) equipped with a four-channel phased-array head coil for signal reception. Routine MRI pulse sequences included axial T1-weighted, T2-weighted and FLAIR. DSC-PWI images were obtained with a T2\*-weighted gradient-echo echoplanar imaging (EPI) sequence (TR/TE 1,490/40 ms, flip angle  $90^\circ$ , FOV  $230 \times 230$  mm, matrix  $128 \times 128$ , 14 sections of thickness 5 mm, acquisition time 78 s) during bolus injection of gadopentetate dimeglumine (DOTAREM®; dose 0.1 mmol/kg body weight, injection rate 4 ml/s), followed by a 20-ml saline flush. A total of 50 measurements were acquired, allowing at least five measurements before bolus arrival. T1-weighted 3D magnetization-prepared rapid acquisition gradient echo (MPRAGE) images (TR/TE 1,840/4.4 ms, section thickness 1 mm, inversion time 110 ms, FOV  $188 \times 250$  mm, matrix  $238 \times 256$ ) were acquired after completion of the DSC sequence.

Parametric maps of rCBV were created from DSC data using the program Stroketool, version 3.1 [29]. Written informed consent was obtained separately for each single imaging modality.

#### Comparative volumetric assessment

F-DOPA PET and MRI imaging studies were automatically coregistered using the commercially available PMOD software, version 3.203/3.403 (PMOD Ltd.). Both PET images and rCBV maps were coregistered to ce-T1-W MR images. If necessary, registration was manually adjusted on all the three axes using anatomic landmarks. The same software was used for semiautomatic contouring of brain tumour volumes on both imaging modalities and for subsequent comparative analysis. Initially, both sets of images were visually scored as positive or negative. Tumour volumes were then estimated for

each modality. Previous studies have shown that tumour-to-background contrast of F-DOPA uptake is similar to that of FET [30, 31]. Therefore, a threshold value of 1.6 over the background uptake was taken as the reference for definition of tumour volume ( $T_{\text{vol } 1.6}$ ), based on the finding of a previous biopsy-controlled study using FET [7]. In case of overlap with basal ganglia uptake, tumour volumes of interest (VOIs) were manually adjusted by two experienced operators in consensus (F.C. and A.P.) to exclude regions of physiological uptake.

To measure mean background uptake, a large region of interest (ROI) was drawn on the unaffected site just above the upper ventricle including both grey and white matter. The same background ROI and threshold value of 1.6 were used to define the tumour volume on CBV maps. This approach was validated in patients with meningioma and then applied to gliomas, as previously described [26]. Manual corrections of the tumour VOI were carefully applied by two experienced operators in consensus (C.P.F. and C.R.E.) to exclude blood vessels whose signal exceeded the cut-off value. The intersection between the tumour VOIs defined on PET images and rCBV maps was calculated using PMOD. The spatial congruence was defined as the percentage of the total tumour volume overlapping between the two sets of studies. For the purpose of this analysis, the total tumour volume was defined as:  $F\text{-DOPA}_{\text{vol } 1.6} + r\text{CBV}_{\text{vol } 1.6} - O_{\text{vol}}$ , where  $F\text{-DOPA}_{\text{vol } 1.6}$  and  $r\text{CBV}_{\text{vol } 1.6}$  are the volumes of pathological signal identified by each modality and  $O_{\text{vol}}$  is the overlapping volume. The hot spots relative to F-DOPA uptake and rCBV were localized semiautomatically and the distance between them calculated.

As previously described [26], a tumour and a reference VOI were defined on morphological MR images to compare tumour-to-background contrast using different functional parameters. The tumour VOI was defined in terms of signal alterations on morphological MR images. In contrast-enhancing tumours ( $n=40$ ) the tumour volume was determined on ce-T1-W images using a visually determined cut-off. In nonenhancing tumours ( $n=10$ ), a spherical VOI of  $10 \text{ cm}^3$  was placed in the centre of signal abnormalities on T1-weighted and T2-weighted images. A large reference VOI was placed on the contralateral hemisphere in an area of normal-appearing brain tissue including white and grey matter. These VOIs were transferred to the coregistered rCBV maps and PET scans and the TBRs were calculated by dividing the mean value of the respective parameter of the tumour VOI by the corresponding mean value of the normal brain VOI. Raw histograms for the tumour VOIs and the reference VOIs were provided for each imaging modality. The maximal pixel values within the tumour VOIs were determined and the raw histograms were normalized to a standardized bin width and a unity of 1 for the curve integral [26].

**Table 1** Patient characteristics, tumour volumes and results of spatial congruence analysis

Patient no.	Study	Gender	Age (years)	Histology	Prior treatments	ce-T1-W volume (ml)	F-DOPA <sub>vol 1.6</sub> (ml)	rCBV <sub>vol 1.6</sub> (ml)	O <sub>vol</sub> (ml)	Spatial congruence (%)
1	Study a	M	41	GBM	S(p), Rt, CHTo	1.08	17.08	1.07	0.004	0.02
	Study b	M	41	GBM	S(p), Rt, CHTo	3.98	7.58	1.81	0.000	0.00
2		M	49	GBM	S(p), Rt, CHTo	23.97	27.05	7.46	0.470	1.38
3		M	69	GBM	S(p), Rt	1.17	10.71 <sup>a</sup>	4.23	2.930	24.39
4		M	53	GBM	S(s), Rt, CHTo	2.64	10.21	0.03	0.020	0.20
5		M	50	GBM	S(b), Rt, CHTo	16.96	37.38	1.41	0.610	1.60
6		M	74	GBM	S(p), Rt, CHTo	0.33	18.27	0.13	0.000	0.00
7		F	52	GBM	S(p), Rt, CHTo	7.15	25.55	26.30	12.510	31.80
8		F	79	GBM	S(t), Rt, CHTo	15.75	43.35	1.91	1.200	2.72
9		F	41	A grade III	S(p), CHT	1.32	22.02	0.12	0.000	0.00
10		F	45	GBM	S(t), Rt, CHTo	0.57	3.78	0.57	0.461	11.84
11		M	64	O grade II	S(p), CHT	3.23	12.16	0.48	0.130	1.04
12		F	51	A grade III	S(p)	0.40	27.55	14.05	5.520	15.30
13		M	55	GBM	S(s), Rt, CHT	11.06	56.22 <sup>a</sup>	6.07	1.870	3.10
14		M	76	GBM <sup>a</sup>	S(b), Rt, CHTo	2.54	50.81 <sup>a</sup>	9.56	8.260	15.85
15		F	49	O grade II	S(p), CHTo	0.00	1.53	0.79	0.000	0.00
16	Study a	M	60	OA grade III	S(s), Rt, CHTo	1.00	3.14	0.21	0.000	0.00
	Study b	M	62	OA grade III	S(s), Rt, CHT	0.00	0.19	1.02	0.000	0.00
17		F	52	DPG	Rt, CHTo	0.65	4.47	0.35	0.350	7.83
18		M	55	A grade II	S(p)	0.55	17.55	10.35	7.860	39.22
19		F	58	O grade III	S(p), Rt, CHTo	3.02	77.73	13.72	11.575	14.49
20		M	44	O grade II	S(p)	0.29	10.22	1.41	0.000	0.00
21		M	53	O grade II	S(p), Rt, CHT	6.84	16.91 <sup>a</sup>	1.40	0.710	4.04
22		F	28	A grade II	S(p)	1.20	9.07	1.95	0.950	9.44
23		M	73	A grade II	S(s)	0.00	1.41	1.30	0.000	0.00
24		M	49	A grade III	S(p), Rt, CHTo	7.09	64.24	3.61	3.330	5.16
25		M	45	DPG	Rt	0.00	5.16	0.00	0.000	0.00
26	Study a	F	47	GBM <sup>a</sup>	S(p), Rt, CHT	0.32	0.30	0.00	0.000	0.00
	Study b	F	46	A grade II	S(p), Rt, CHTo	0.27	1.52 <sup>a</sup>	0.03	0.000	0.00
27	Study a	F	54	A grade III	S(s), Rt, CHTo	2.80	7.09	0.95	0.052	0.65
	Study b	F	56	A grade III	S(s), Rt, CHTo	4.70	2.98	0.21	0.000	0.00
28		M	54	A grade III	S(p), Rt, CHTo	5.73	29.93	3.17	2.732	9.00
29		M	58	A grade III	S(b), Rt, CHT	0.42	3.82	0.37	0.206	5.18
30	Study a	F	43	A grade II	S(s), S(p), CHTo	1.78	0.16	0.44	0.000	0.00
	Study b	F	45	GBM <sup>a</sup>	S(s), S(p), Rt, CHTo	3.71	18.60	0.93	0.925	4.97

**Table 1** (continued)

Patient no.	Gender	Age (years)	Histology	Prior treatments	ce-T1-W volume (ml)	F-DOPA <sub>vol 1.6</sub> (ml)	rCBV <sub>vol 1.6</sub> (ml)	O <sub>vol</sub> (ml)	Spatial congruence (%)
31	M	34	A grade III	S(p), Rt, CHTo	11.16	18.78 <sup>b</sup>	1.89	1.760	9.31
32	M	33	A grade III	S(p), Rt, CHTo	4.12	20.38 <sup>a</sup>	3.52	0.500	2.14
33	F	30	GA grade III	S(t), CHTo	6.05	38.07	0.59	0.590	1.55
34	M	22	GLM	S(b)	0.00	19.12	7.17	2.920	12.49
35	M	36	GBM	S(p), Rt, CHT	2.72	3.67 <sup>b</sup>	0.00	0.000	0.00
36	M	45	GLM	S(p)	0.00	70.97 <sup>b</sup>	7.02	1.070	1.39
37	M	47	O grade II	S(b)	0.00	46.59 <sup>b</sup>	0.35	0.000	0.00
38	M	42	GLM	S(b)	0.00	220.95 <sup>b</sup>	0.44	0.439	0.20
39	F	47	A grade III	S(p), Rt, CHTo	1.96	39.70 <sup>b</sup>	7.57	5.210	12.39
40	M	65	GBM	S(t), Rt, CHTo	0.26	0.06	0.98	0.010	0.97
41	M	66	GBM	S(b), Rt, CHT	0.15	0.00	0.00	0.000	Not applicable
42	F	54	GBM	S(p), Rt, CHTo	0.41	5.36 <sup>a</sup>	7.07	0.718	6.13
43	Study a Study b	64 65	OA grade II GBM <sup>a</sup>	S(s), Rt, CHTo S(s), Rt, CHT	0.00 2.68	0.08 0.01	0.00 2.13	0.000 0.000	0.00 0.00
44	M	19	DPG	Rt, CHTo	0.00	0.16	0.52	0.000	0.00

*Histological subtypes: GBM* glioblastoma; *GLM* gliomatosis cerebri; *DPG* diffuse pontine glioma (histologically unverified); *A* astrocytoma; *O* oligodendroglioma; *OA* oligoastrocytoma; *GA* ganglioglioma. *Prior treatments: S(t)* surgery, total resection; *S(s)* surgery, subtotal (>90 %) resection; *S(p)* surgery, partial (<90 %) resection; *S(b)* biopsy; *Rt* radiotherapy; *CHT* chemotherapy; *CHTo* ongoing chemotherapy

<sup>a</sup> Patients with physiological radioactivity of the basal ganglia touched, but not clearly infiltrated, by tumour

<sup>b</sup> Patients with a large infiltration of the basal ganglia by tumour

## Statistical analysis

The Statistical Package for the Social Sciences (SPSS, vers. 20; SPSS Inc., Chicago, IL) was used for statistical analysis. For comparison between groups, Student's *t* test and the Mann-Whitney *U* test were used for normally and non-normally distributed variables, respectively. For correlation analysis, Pearson's *r* was used. Probability values of less than 0.05 were considered significant.

## Results

The patient characteristics, together with tumour volumes and results of spatial congruence analysis are shown in Table 1.

### Comparative volumetric assessment

On visual inspection, 49 of 50 F-DOPA PET and 45 of 50 CBV studies were classified as positive. In one patient both studies were negative, while in four patients the PET study was positive and the CBV study was negative.  $F-DOPA_{vol\ 1.6}$  greatly exceeded  $rCBV_{vol\ 1.6}$  ( $p < 0.00001$ ; Fig. 1). No correlation was found between  $F-DOPA_{vol\ 1.6}$  and  $rCBV_{vol\ 1.6}$  ( $r = 0.19$ ,  $p = 0.17$ ). In the overall population, the median  $F-DOPA_{vol\ 1.6}$  was 11.44 ml (range 0 – 220.95 ml) and the median  $rCBV_{vol\ 1.6}$  was 1.04 ml (range 0 – 26.30 ml). High-grade gliomas had a significantly larger  $F-DOPA_{vol\ 1.6}$  than low-grade gliomas (median  $F-DOPA_{vol\ 1.6}$  18.69 ml and 4.81 ml in high-grade and low-grade gliomas, respectively,  $p = 0.023$ ), while only a trend toward significance was observed for  $rCBV_{vol\ 1.6}$  (median  $rCBV_{vol\ 1.6}$  1.61 ml

and 0.5 ml in high-grade and low-grade gliomas, respectively,  $p = 0.071$ ).

The overall median total tumour volume was 12.26 ml (18.75 and 4.81 in high-grade and low-grade gliomas, respectively,  $p = 0.019$ ). The percent contributions to the total tumour volume were 89.95 % and 5.61 % for F-DOPA uptake and rCBV, respectively (Fig. 2). The median  $O_{vol}$  was 0.28 ml in the overall population (0.49 ml and 0 ml in high-grade and low-grade gliomas, respectively,  $p = 0.025$ ). This, in turn, resulted in an overall median spatial congruence of 1.38 % (range 0 – 39.22 %). No significant differences were found in terms of spatial congruence between high-grade and low-grade gliomas ( $p = 0.061$ ). Table 2 summarizes the results of comparative volumetric assessment.

### Location of hot spots on F-DOPA PET and rCBV studies

Including only positive studies, the mean radial distance between F-DOPA uptake and rCBV tumour hot spots was  $27.17 \pm 16.92$  mm (range 2.24 – 64.8 mm). There were no differences in hot-spot distance between high-grade and low-grade gliomas ( $p = 0.93$ ).

### Tumour-to-brain ratios

TBRs were significantly higher on F-DOPA PET studies than on rCBV studies (overall mean TBR  $1.76 \pm 0.60$  and  $1.15 \pm 0.52$  for F-DOPA uptake and rCBV, respectively,  $p < 0.0001$ ; Fig. 3). No differences in TBRs were found between high-grade and low-grade gliomas ( $p = 0.36$  and  $p = 0.09$  for rCBV and F-DOPA uptake, respectively).

### Comparison of histograms

The histograms of F-DOPA uptake allowed a clear separation of tumour from background, whereas separation based on histograms of rCBV was poor (Fig. 4).

## Discussion

Among the imaging modalities complementary to conventional MRI, amino acid PET and PWI are often seen as competitors. Amino acid PET, especially when short half-life emitters such as  $^{11}C$  are employed, presents some logistic difficulties, while PWI images have the clear advantage of being easily obtained in a single MRI session. However, the biological mechanisms explored and the information provided are inherently different, as shown in the present study, which

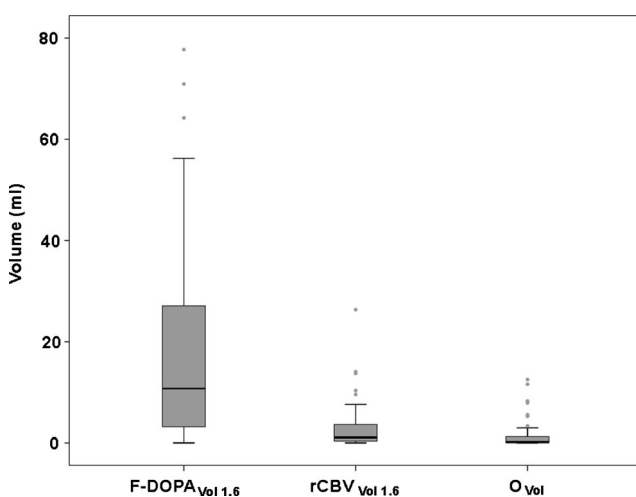


**Fig. 1** Box-plot of  $F-DOPA_{vol\ 1.6}$  and  $rCBV_{vol\ 1.6}$  values and the total overlapping volumes ( $O_{vol}$ ). The plots include data from the overall study population with one outlier excluded (patient 38,  $F-DOPA_{vol\ 1.6}$  220.95 ml)

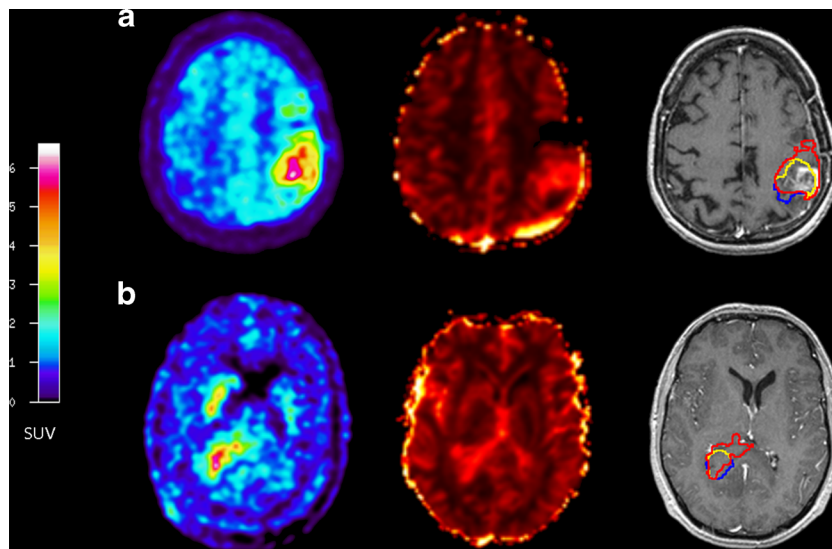


**Fig. 2** Examples of spatial congruence between tumour volumes derived from F-DOPA PET and rCBV images. These studies were chosen from among those with the largest volume overlap. *Left to right*: axial F-DOPA PET, rCBV and contrast-enhanced T1-weighted images with superimposition of tumour VOIs (*red* F-DOPA-derived tumour volume, *blue* rCBV-

derived tumour volume, *yellow* overlapping volume). **a** Patient 7, glioblastoma: F-DOPA<sub>vol 1.6</sub> and rCBV<sub>vol 1.6</sub> are similar (25.55 ml and 26.30 ml, respectively); spatial congruence 31.8 %. **b** Patient 34, noncontrast-enhancing gliomatosis cerebri: F-DOPA<sub>vol 1.6</sub> and rCBV<sub>vol 1.6</sub> are 19.12 ml and 7.17 ml, respectively; spatial congruence 12.49 %

confirmed and extended to F-DOPA the findings of a previous study of FET [26].

The first most relevant finding of our study is that the regions with increased F-DOPA uptake were much larger than those with increased rCBV values (Fig. 1). In addition, we were able to confirm that TBRs are significantly higher for F-DOPA uptake than for rCBV maps (Fig. 3), indicating that F-DOPA uptake is superior to rCBV for differentiating between tumour and normal brain, as also reflected by the histogram analysis (Fig. 4) [26]. No significant differences in TBR were found between high-grade and low-grade gliomas, consistent with the results of a previous study showing a failed correlation between F-DOPA uptake and tumour grade in patients with previously treated glioma [32]. Although there might be some degree of nonspecific uptake [33], the larger

tumour volumes seen on F-DOPA PET in both enhancing and nonenhancing regions seem to correlate better with the real tumour extent, as already suggested by previous studies [5–16].

Taken together, these findings suggest that the diagnostic yield of amino acid PET is greater than that of PWI, in contradiction to the findings of some studies indicating that radionuclide imaging could be replaced by PWI [22–25]. In those studies, however, relatively small ROIs were chosen in tumours and normal brain regions and often a binary interpretation of rCBV was used (positive vs. negative) for comparison with amino acid uptake. In our opinion, this approach is unlikely to give correct information as to total tumour volume and might be better suited to other clinical issues, e.g. the differential diagnosis between radiation-induced changes and

**Table 2** Volumetric analysis, together with mean values and standard deviations for all the studies, in order to facilitate comparison with the findings of Filss et al. [26]

	ce-T1-W volume (ml) <sup>a</sup>	F-DOPA <sub>vol1.6</sub> (ml) <sup>a</sup>	rCBV <sub>vol1.6</sub> (ml)	Total tumour volume (ml) <sup>a</sup>	O <sub>vol</sub> (ml) <sup>a</sup>	F-DOPA only (%)	rCBV only (%)	Spatial congruence (%) <sup>a</sup>
All studies (n=50)								
Median	1.18	11.44	1.04	12.26	0.28	89.95	5.61	1.38
Mean ± SD	3.24±4.9	22.59±34.9	3.13±4.8	24.20±35.2	1.51±2.9	78.10±27.1	16.67±26.5	5.21±8.4
High-grade (n=36)	2.53	18.69	1.61	18.75	0.49	89.95	5.61	1.60
Low-grade (n=14)	0.27	4.81	0.50	4.81	0	89.96	6.90	0

Not all variables were normally distributed

<sup>a</sup> Variables for which the difference between high-grade and low-grade gliomas was statistically significant (Mann-Whitney *U* test)

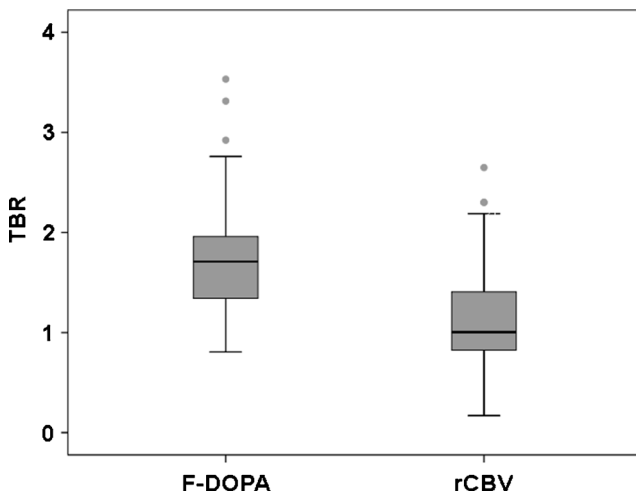


**Fig. 3** Box-plot of tumour-to-brain ratios (*TBR*) of F-DOPA uptake and rCBV. The mean *TBR* of F-DOPA uptake is significantly higher than rCBV *TBR* (1.76 vs. 1.14,  $p < 0.0001$ , two-tailed Student's *t* test)

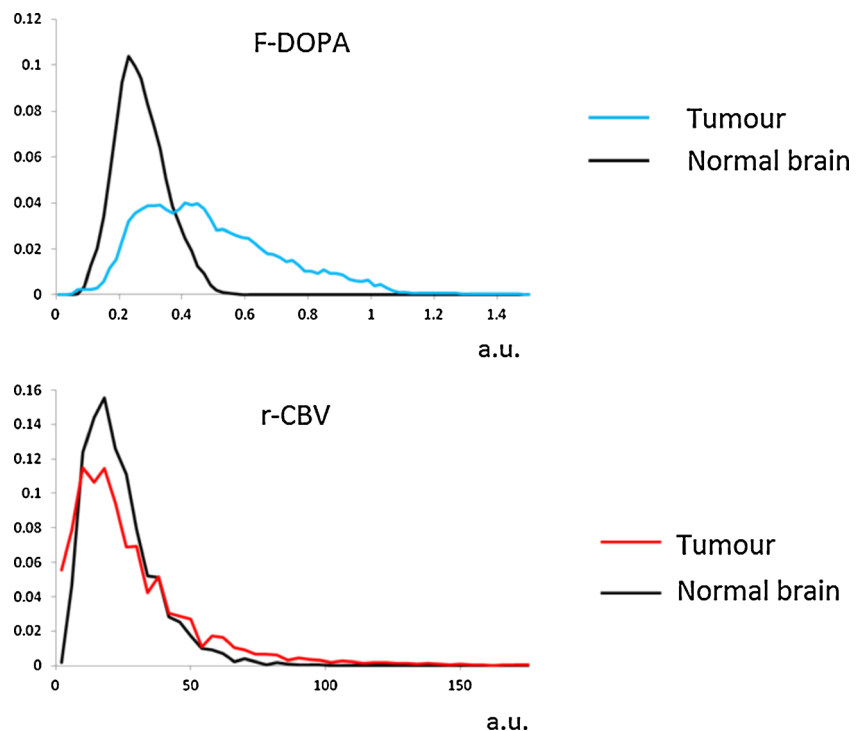
recurrent or progressive brain metastases, where the tumour volume is well defined and a binary response is required. To overcome these limitations, we applied a volumetric approach to the imaging data here, using large reference VOIs, the same threshold values and automatic segmentation methods for both F-DOPA PET and PWI images. This method has been validated and discussed elsewhere [26].

The second major result of our study was the poor spatial congruence between F-DOPA uptake and rCBV. Following its

definition, the spatial congruence was negatively influenced by large difference between volumes identified by the two imaging modalities. It should be noted, however, that although  $rCBV_{vol 1.6}$  contributed only a small fraction to the total tumour volume, it was usually not entirely confined within  $F-DOPA_{vol 1.6}$ . Additionally, a further spatial congruence analysis revealed that the overlap between  $rCBV_{vol 1.6}$  and contrast enhancement on ce-T1-W sequences was also small (data not shown). This means that F-DOPA PET and PWI should be considered as complementary rather than mutually exclusive, in line with the conclusion of a recent study showing that MET PET and PWI provide complementary baseline data in low-grade gliomas [34]. The authors, however, found that hot spot regions of MET uptake and rCBV coincided in all cases, whereas in the present study the mean radial distance between F-DOPA uptake and rCBV hot spots was 27.17 mm. In our study, we could not confirm such coincidence, and we argue that the large discrepancy between our results and those of Berntsson et al. [34] can be explained by differences in patient characteristics, in particular by the fact that all our patients had received previous treatment. Interestingly, almost the same mean radial hot spot distance (25.39 mm) was found in patients imaged with FET [26].

Overall, our results compare well with those of a previous similar study investigating FET [26]. In our cohort, median spatial congruence was 1.38 % vs. 5.6 % reported previously with FET (see online supplementary material of [26]). Since the same methodology was employed in both studies, the

**Fig. 4** Mean histograms of tumour and normal brain F-DOPA uptake signal and rCBV signal. F-DOPA uptake allows better separation of tumour from normal brain than rCBV





small discrepancy probably reflects the different inclusion criteria (30 of 56 patients in the study of Filss et al. [26] were untreated) and slightly different overall tumour volumes.

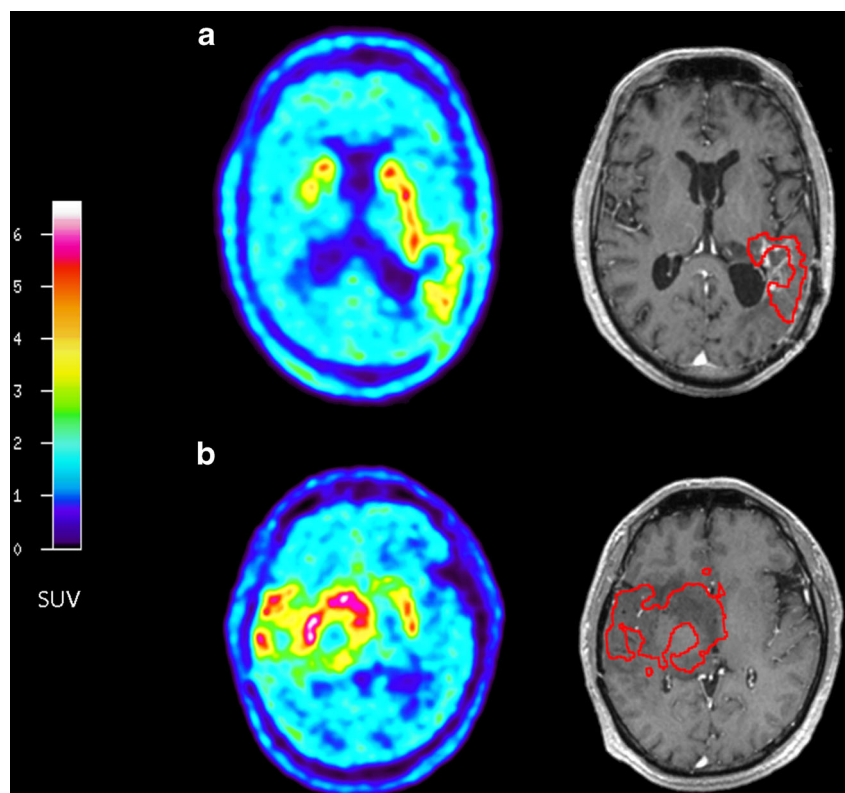
We are aware that this study had several limitations, including its retrospective nature and the broad range of tumour stage and prior treatment history. Furthermore, histopathology was performed as part of the usual standard of care and no targeted biopsies were taken to evaluate the discrepancies between F-DOPA PET and rCBV in more detail. Our conclusions are based primarily on the well-known ability of radiolabelled amino acids to reflect the extent of gliomas reliably. Therefore, a biopsy-controlled study is needed to confirm our findings. Since a well-established threshold for separating tumour from nontumour tissue in terms of rCBV does not exist, we used the same threshold as for F-DOPA in order to be able to compare the two imaging methods. However, one might argue that the main objective of PWI is not to define the whole tumour extent but, instead, to detect tumour subregions suggestive of high-grade malignant tumour tissue [17]. Nevertheless, in our opinion this approach can be reproduced easily and reduces to a reasonable extent the large variability in the subjective interpretation criteria of rCBV maps.

Furthermore, F-DOPA PET imaging itself is not free from drawbacks. Although single transport mechanisms are not known in detail and might show some peculiarities, no major

differences have been found among the available amino acids in terms of tumour detection [30, 31, 35]. However, F-DOPA is a substrate for the enzyme aromatic amino acid decarboxylase, found in high abundance in dopaminergic neurons, and therefore shows physiological uptake in the basal ganglia [36]. This uptake represents a known pitfall of F-DOPA since it may interfere with tumour uptake, as in 6 of the 50 studies (12 %) in our patient cohort in which the striatal uptake prevented precise tumour delineation (Fig. 5). This problem probably did not affect the overall results of the study, but it should be born in mind that with F-DOPA the tumour volume might be difficult to evaluate in a nonnegligible number of patients. In such patients in particular integration with other imaging modalities and/or an alternative amino acid probe would be required.

In conclusion, this study demonstrated that the information provided by F-DOPA PET and rCBV maps is substantially different in patients with recurrent or progressive glioma. Image interpretation is easier and a larger tumour extent is identified with F-DOPA PET than with rCBV maps. The integration of new imaging techniques might help the assessment of response to treatment and radiotherapy planning. However, the significance of different tumour regions delineated with these techniques needs to be explored in prospective studies.

**Fig. 5** Patterns of interference between physiological basal ganglia uptake and tumour delineation. **a** Tumour uptake with no infiltration of the striatum (patient 21). The pathological signal does not overlap with basal ganglia activity and a clear distinction is still possible. **b** The tumour largely displaces and infiltrates the basal ganglia (patient 36), and the separation of pathological and physiological signal is difficult. In both **a** and **b**, tumour VOIs are shown



## Compliance with Ethical Standards

**Conflicts of interest** None.

**Ethical approval** All procedures performed in the study were in accordance with the standards of the institutional ethical committee and with the 1964 Helsinki Declaration and its later amendments or comparable ethical standards. This article does not contain any studies with animals performed by any of the authors.

**Informed consent** Informed consent was obtained from all individual participants included in the study.

## References

- Wen PY, Macdonald DR, Reardon DA, Cloughesy TF, Sorensen AG, Galanis E, et al. Updated response assessment criteria for high-grade gliomas: response assessment in neuro-oncology working group. *J Clin Oncol*. 2010;28:1963–72.
- Yang I, Aghi MK. New advances that enable identification of glioblastoma recurrence. *Nat Rev Clin Oncol*. 2009;6:648–57.
- Heiss WD, Raab P, Lanfermann H. Multimodality assessment of brain tumors and tumor recurrence. *J Nucl Med*. 2011;52:1585–600.
- Langen KJ, Bröer S. Molecular transport mechanisms of radiolabeled amino acids for PET and SPECT. *J Nucl Med*. 2004;45:1435–6.
- Arbizu J, Tejada S, Marti-Climent JM, Diez-Valle R, Prieto E, Quincoces G, et al. Quantitative volumetric analysis of gliomas with sequential MRI and 11C-methionine PET assessment: patterns of integration in therapy planning. *Eur J Nucl Med Mol Imaging*. 2012;39:771–81.
- Kracht LW, Miletic H, Busch S, Jacobs AH, Voges J, Hoevels M, et al. Delineation of brain tumor extent with [11C]L-methionine positron emission tomography: local comparison with stereotactic histopathology. *Clin Cancer Res*. 2004;10:7163–70.
- Pauleit D, Floeth F, Hamacher K, Riemenschneider MJ, Reifemberger G, Müller HW, et al. O-(2-[18F]fluoroethyl)-L-tyrosine PET combined with MRI improves the diagnostic assessment of cerebral gliomas. *Brain*. 2005;128:678–87.
- Pafundi DH, Laack NN, Youland RS, Parney IF, Lowe VJ, Giannini C, et al. Biopsy validation of 18F-DOPA PET and biodistribution in gliomas for neurosurgical planning and radiotherapy target delineation: results of a prospective pilot study. *Neuro Oncol*. 2013;15:1058–67.
- Galldiks N, Stoffels G, Ruge MI, Rapp M, Sabel M, Reifemberger G, et al. Role of O-(2-18F-fluoroethyl)-L-tyrosine PET as a diagnostic tool for detection of malignant progression in patients with low-grade glioma. *J Nucl Med*. 2013;54:2046–54.
- Jansen NL, Suchorska B, Wenter V, Eigenbrod S, Schmid-Tannwald C, Zwergal A, et al. Dynamic 18F-FET PET in newly diagnosed astrocytic low-grade glioma identifies high-risk patients. *J Nucl Med*. 2014;55:198–203.
- Galldiks N, Langen KJ, Holy R, Pinkawa M, Stoffels G, Nolte KW, et al. Assessment of treatment response in patients with glioblastoma using O-(2-18F-fluoroethyl)-L-tyrosine PET in comparison to MRI. *J Nucl Med*. 2012;53:1048–57.
- Harris RJ, Cloughesy TF, Pope WB, Nghiemphu PL, Lai A, Zaw T, et al. 18F-FDOPA and 18F-FLT positron emission tomography parametric response maps predict response in recurrent malignant gliomas treated with bevacizumab. *Neuro Oncol*. 2012;14:1079–89.
- Galldiks N, Rapp M, Stoffels G, Fink GR, Shah NJ, Coenen HH, et al. Response assessment of bevacizumab in patients with recurrent malignant glioma using [18F]fluoroethyl-L-tyrosine PET in comparison to MRI. *Eur J Nucl Med Mol Imaging*. 2013;40:22–33.
- Pirotte BJ, Levivier M, Goldman S, Massager N, Wikler D, Dewitte O, et al. Positron emission tomography-guided volumetric resection of supratentorial high-grade gliomas: a survival analysis in 66 consecutive patients. *Neurosurgery*. 2009;64:471–81.
- Nuutinen J, Sonninen P, Lehtikainen P, Sutinen E, Valavaara R, Eronen E, et al. Radiotherapy treatment planning and long-term follow-up with [(11)C]methionine PET in patients with low-grade astrocytoma. *Int J Radiat Oncol Biol Phys*. 2000;48:43–52.
- Piroth MD, Holy R, Pinkawa M, Stoffels G, Kaiser HJ, Galldiks N, et al. Prognostic impact of postoperative, pre-irradiation (18)F-fluoroethyl-L-tyrosine uptake in glioblastoma patients treated with radiochemotherapy. *Radiother Oncol*. 2011;99:218–24.
- Law M, Young RJ, Babb JS, Peccerelli N, Cheang S, Gruber ML, et al. Gliomas: predicting time to progression or survival with cerebral blood volume measurements at dynamic susceptibility-weighted contrast-enhanced perfusion MR imaging. *Radiology*. 2008;247:490–8.
- Barajas Jr RF, Chang JS, Segal MR, Parsa AT, McDermott MW, Berger MS, et al. Differentiation of recurrent glioblastoma multiforme from radiation necrosis after external beam radiation therapy with dynamic susceptibility-weighted contrast-enhanced perfusion MR imaging. *Radiology*. 2009;253:486–96.
- Hu LS, Eschbacher JM, Heiserman JE, Dueck AC, Shapiro WR, Liu S, et al. Reevaluating the imaging definition of tumor progression: perfusion MRI quantifies recurrent glioblastoma tumor fraction, pseudoprogression, and radiation necrosis to predict survival. *Neuro Oncol*. 2012;14:919–30.
- Aronen HJ, Gazit IE, Louis DN, Buchbinder BR, Pardo FS, Weisskoff RM, et al. Cerebral blood volume maps of gliomas: comparison with tumor grade and histologic findings. *Radiology*. 1994;191:41–51.
- Barajas Jr RF, Phillips JJ, Parvataneni R, Molinaro A, Essock-Burns E, Boume G, et al. Regional variation in histopathologic features of tumor specimens from treatment-naïve glioblastoma correlates with anatomic and physiologic MR imaging. *Neuro Oncol*. 2012;14:942–54.
- Sadeghi N, Salmon I, Decaestecker C, Levivier M, Metens T, Wikler D, et al. Stereotactic comparison among cerebral blood volume, methionine uptake, and histopathology in brain glioma. *AJNR Am J Neuroradiol*. 2007;28:455–61.
- Dandois V, Rommel D, Renard L, Jamart J, Cosnard G. Substitution of 11C-methionine PET by perfusion MRI during the follow-up of treated high-grade gliomas: preliminary results in clinical practice. *J Neuroradiol*. 2010;37:89–97.
- Kim YH, Oh SW, Lim YJ, Park CK, Lee SH, Kang KW, et al. Differentiating radiation necrosis from tumor recurrence in high-grade gliomas: assessing the efficacy of 18F-FDG PET, 11C-methionine PET and perfusion MRI. *Clin Neurol Neurosurg*. 2010;112:758–65.
- Tietze A, Boldsen JK, Mouridsen K, Ribe L, Dyve S, Cortnum S, et al. Spatial distribution of malignant tissue in gliomas: correlations of 11C-L-methionine positron emission tomography and perfusion- and diffusion-weighted magnetic resonance imaging. *Acta Radiol*. 2014. doi:10.1177/0284185114550020.
- Filss CP, Galldiks N, Stoffels G, Sabel M, Wittsack HJ, Turowski B, et al. Comparison of 18F-FET PET and perfusion-weighted MR imaging: a PET/MR imaging hybrid study in patients with brain tumors. *J Nucl Med*. 2014;55:540–5.
- Louis DN, Ohgaki H, Wiestler OD, Cavenee WK, Burger PC, Jouvet A, et al. The 2007 WHO classification of tumours of the central nervous system. *Acta Neuropathol*. 2007;114:97–109.
- Stupp R, Mason WP, van den Bent MJ, Weller M, Fisher B, Taphoorn MJ, et al. Radiotherapy plus concomitant and adjuvant temozolomide for glioblastoma. *N Engl J Med*. 2005;352:987–96.

29. Wittsack HJ, Ritzl A, Mödder U. User friendly analysis of MR investigations of the cerebral perfusion: windows(R)-based image processing. *Rofo*. 2002;174:742–6. Article in German.
30. Kratochwil C, Combs SE, Leotta K, Afshar-Oromieh A, Rieken S, Debus J, et al. Intra-individual comparison of 18F-FET and 18F-DOPA in PET imaging of recurrent brain tumors. *Neuro Oncol*. 2014;16:434–40.
31. Lapa C, Linsenmann T, Monoranu CM, Samnick S, Buck AK, Bluemel C, et al. Comparison of the amino acid tracers 18F-FET and 18F-DOPA in high-grade glioma patients. *J Nucl Med*. 2014;55:1611–6.
32. Fueger BJ, Czernin J, Cloughesy T, Silverman DH, Geist CL, Walter MA, et al. Correlation of 6-18F-fluoro-L-dopa PET uptake with proliferation and tumor grade in newly diagnosed and recurrent gliomas. *J Nucl Med*. 2010;51:1532–8.
33. Hutterer M, Nowosielski M, Putzer D, Jansen NL, Seiz M, Schocke M, et al. [18F]-fluoro-ethyl-L-tyrosine PET: a valuable diagnostic tool in neuro-oncology, but not all that glitters is glioma. *Neuro Oncol*. 2013;15:341–51.
34. Berntsson SG, Falk A, Savitcheva I, Godau A, Zetterling M, Hesselager G, et al. Perfusion and diffusion MRI combined with 11C-methionine PET in the preoperative evaluation of suspected adult low-grade gliomas. *J Neurooncol*. 2013;114:241–9.
35. Becherer A, Karanikas G, Szabó M, Zetting G, Asenbaum S, Marosi C, et al. Brain tumour imaging with PET: a comparison between [18F]fluorodopa and [11C]methionine. *Eur J Nucl Med Mol Imaging*. 2003;30:1561–7.
36. Schiepers C, Chen W, Cloughesy T, Dahlbom M, Huang SC. 18F-FDOPA kinetics in brain tumors. *J Nucl Med*. 2007;48:1651–61.